790 *Macromolecules* **2010**, *43*, 790–796
DOI: 10.1021/ma902028u

Macromolecules
ARTICLE

Effect of Ionic Liquid on Mechanical Properties and Morphology of Zwitterionic Copolymer Membranes

Rebecca H. Brown,[†] Andrew J. Duncan,[†,‡] Jae-Hong Choi,[§] Jong Keun Park,[†] Tianyu Wu,[†] Donald J. Leo,[‡] Karen I. Winey,[§] Robert B. Moore,[†] and Timothy E. Long*,[†]

[†]*Department of Chemistry, Virginia Tech, Blacksburg, Virginia 24061,* [‡]*Department of Mechanical Engineering (CIMSS), Virginia Tech, Blacksburg, Virginia 24061, and* [§]*Department of Materials Science and Engineering, University of Pennsylvania, Philadelphia, Pennsylvania 19104*

Received September 11, 2009; Revised Manuscript Received December 1, 2009

ABSTRACT: Zwitterionomers containing less than 13 mol % zwitterion functionality were synthesized using free radical copolymerization of *n*-butyl acrylate (nBA) and sulfobetaine monomers. X-ray scattering results revealed a two-phase morphology, which is typical of random ionomers with an ionomer peak at $q \sim 1.5$ nm^{-1}. Swelling studies in the ionic liquid (IL), 1-ethyl-3-methylimidazolium ethylsulfate (EMIm ES), showed an influence of zwitterionic structure on IL uptake. Zwitterionomer membranes were swollen to various IL contents, and the influence of IL on mechanical properties, morphology, and ionic conductivity was explored through dynamic mechanical analysis (DMA), X-ray scattering, and impedance spectroscopy, respectively. Results revealed that IL preferentially swelled the zwitterionic domains but was excluded from the matrix phase. Significant changes in mechanical properties and ionic conductivity were observed above a critical uptake of IL. Fundamental explorations of the interaction of ILs with sulfobetaine-containing copolymers may lead to the use of zwitterionomers in emerging membrane applications.

Introduction

Polybetaines are a class of zwitterionic polymers featuring a covalently bound cation and anion on each repeating unit. The presence of two oppositely charged groups bound in close proximity creates a large dipole moment, lending many unique properties to the betaine structure. Zwitterionic structures based on ammonioalkanesulfonates (sulfobetaines) have received significant attention from Galin and others due to their high dipole moments, reported as $\mu \sim 18.7-27.6$ D.[1] These chemical structures are stable over a wide range of temperatures and feature permanent charge over a large pH range. Polymeric betaines exhibit remarkable miscibility with various inorganic and metal salts up to stoichiometric quantities.[2−4] These salt−polyzwitterion mixtures formed amorphous blends due to strong ion−dipole interactions that precluded salt segregation or crystallization within the zwitterion matrix for a variety of different inorganic salts. This unique ability to dissolve large amounts of salts has sparked interest in polyzwitterions as polymeric host matrices for polar guest molecules.[4]

While polymeric betaines, especially sulfobetaines and phosphobetaines, are extensively studied in the literature for a variety of aqueous applications,[5,6] considerably less attention has been devoted to the performance and application of random copolymers featuring zwitterionic sites within hydrophobic matrices. Galin and co-workers[7,8] introduced copolymers of sulfobetaines with 2-ethoxyethyl acrylate as a new class of low-T_g ionomers for biphasic materials with properties potentially better than cationic ionomers of similar structure. Subsequent studies with copolymers containing a poly(*n*-butyl acrylate) (PnBA) matrix confirmed that zwitterionic copolymers exhibited mechanical properties and morphologies similar to classical ionomers.[9−12] Detailed structural and morphological analysis revealed a morphology in agreement with the EHM model,[13] where increasing zwitterionic content led to development of a phase-separated system with a second high temperature T_g representing overlapping regions of restricted mobility surrounding phase-separated multiplets.[11]

Ionic liquids (ILs) have become increasingly important in recent years for applications spanning many fields of chemistry. ILs are molten salts that are liquids below 100 °C and exhibit excellent properties including chemical and thermal stability, low vapor pressure, and high ionic conductivity.[14] Although widely used as solvents for synthesis and extractions, ILs are also used as diluents in polymeric membranes to afford high conductivities for applications including lithium batteries,[15,16] solar cells,[14,17,18] and electromechanical transducers.[19−23] For example, replacing water with an IL as the diluent in Nafion membranes for ionic polymer transducers resulted in an increase from 30 000 cycles to more than 250 000 cycles.[24] This drastic change was due to a lack of solvent evaporation for ILs, which led to deterioration of transducer performance after 30 000 cycles with water as the diluent.

The goal of the present study is to explore the interaction of ionic liquids with low-T_g zwitterionomers featuring moderate loadings of dipolar sulfobetaine-based zwitterions. ILs are expected to interact with the zwitterion functionality in a similar fashion to inorganic salts or polar liquids (water, glycerol, ethylammonium nitrate) as previously reported.[25] DMA, SAXS, and impedance spectroscopy are employed to determine the partitioning of IL within the zwitterionic membrane as well as its effects on polymer morphology. Incorporation of ILs with high ionic conductivities into zwitterion-containing copolymers may have implications in the use of zwitterionomer membranes in electronic devices, where the lack of mobile counterions in the membrane serves as a fundamental difference from current ionomers.

Experimental Section

Materials. Zwitterionic monomers, *N*-(3-sulfopropyl)-*N*-methacryloxyethyl-*N*,*N*-dimethylammonium betaine (SBMA) and *N*-(3-sulfopropyl)-*N*-methacryloylamidopropyl-*N*,*N*-dimethylammonium betaine (SBMAm) were generously provided

*To whom correspondence should be addressed.

 Published on Web 12/16/2009 © 2009 American Chemical Society

by Raschig GMBH and used without purification. Dimethyl sulfoxide (DMSO, 99.9+%), azobis(isobutyronitrile) (AIBN), and *n*-butyl acrylate (nBA) were purchased from Sigma-Aldrich Chemical Co. AIBN was recrystallized from methanol. *n*-Butyl acrylate (nBA) was passed through a neutral alumina column and distilled under reduced pressure from CaH_2. Chloroform (Optima grade) was purchased from Fisher Scientific and used without further purification. 1-Ethyl-3-methylimidazolium ethylsulfate (EMIm ES) was purchased from Alfa Aesar and stored over molecular sieves.

Synthesis of Sulfobetaine Methacrylate-*co*-Butyl Acrylate Copolymers. A typical copolymerization is described. nBA (13.4 g, 0.105 mol) and SBMA (3.26 g, 0.012 mol) were added to a 250 mL, round-bottomed flask equipped with a magnetic stir bar. The reaction mixture was diluted with DMSO (137 mL, 90 wt %), and AIBN (83 mg, 0.50 wt %) was added to the reaction vessel. The reaction was sparged with N_2 for 15 min and placed in an oil bath at 60 °C for 24 h. The polymer was precipitated into 4 L of water and dried under reduced pressure. Residual DMSO was removed with reduced pressure (0.4 mmHg) at 60 °C. The isolated polymer was dried under reduced pressure at 80 °C for 48 h and stored in a desiccator. Complete removal of residual monomers was confirmed with the disappearance of characteristic vinylic peaks in the ^{1}H NMR spectrum. Sulfobetaine methacrylamide-*co*-butyl acrylate copolymers (PnBA-*co*-PSBMAm) were synthesized and purified under similar conditions, according to previously reported methods.[26] Typical yields following polymerization and isolation were ~75%. Although reactivity ratios were not determined for this monomer pair, the thermal, mechanical, and morphological analysis suggests a uniform copolymerization process.

Membrane Preparation and Swelling in Ionic Liquid. Films were solution cast from chloroform (0.1 g/mL) into Teflon molds to achieve a thickness of 0.25−0.30 mm. Films were dried at room temperature overnight and then heated at 80 °C for 72 h under vacuum prior to characterization or treatment. Dry films were cut into strips approximately 20 mm × 5 mm. Film pieces were immersed in EMIm ES and stored in sealed glass vials inside a desiccator maintained at 20% relative humidity (RH). Film pieces were periodically weighed to determine the uptake of IL. Films were removed using forceps and blotted with a Kimwipe to remove excess EMIm ES on the polymer surface. IL uptake was calculated according to the following equation: % uptake = $(m - m_0)/m_0$, where m_0 is the initial dry film mass and m is the mass of the swollen film at a given time. IL uptake is also reported as a molar ratio of EMIm ES relative to the number of zwitterionic units in the membrane.

Instrumentation. ^{1}H NMR spectra of the polymers were obtained on a Varian Unity 400 MHz spectrometer in $CDCl_3$. Molar compositions of the polymers were determined by comparison of shifts at 1.0 ppm for the $-CH_3$ on nBA with the $-CH_3$ groups on the quaternary ammonium of the sulfobetaine unit at 3.20 ppm.[27] Size exclusion chromatography (SEC) was used to determine the molecular weights of zwitterionomers at 50 °C in *N*,*N*-dimethyformamide (DMF) with 0.01 M lithium bromide (LiBr) at 1 mL min^{-1}. DMF SEC was performed on a Waters SEC equipped with two Waters Styragel HR5E (DMF) columns, a Waters 717plus autosampler, and a Waters 2414 differential refractive index detector. Reported molecular weights are relative to polystyrene standards. Dynamic mechanical analysis (DMA) measurements were performed on a TA Instruments Q800 dynamic mechanical analyzer in tension mode at a frequency of 1 Hz and a temperature ramp of 3 °C min^{-1} over the range −90 to 150 °C. Transitions are reported as peak values in the loss modulus.

Electrical impedance spectroscopy (EIS) was performed with an Autolab PGSTAT12 potentiostat/galvanostat with FRA2 impedance module from 1 MHz to 0.1 Hz. The instrument was operated in potentiostatic mode to apply a single 100 mV rms sine wave while measuring the complex impedance response of the sample. A custom fixture aligned two parallel rectangular brass rods at a defined separation of 0.3 cm to allow for in-plane impedance measurements. Ionic conductivity values (σ, S/cm) were calculated according to $\sigma = t/(Rlw)$, where R is the bulk membrane resistance (ohms), t (cm) is the sample thickness, l (cm) is the sample length, and w (cm) is the sample width. The kinetic portion of the complex impedance data (Nyquist plot) was fit with a semicircle to extrapolate the membrane resistance as the low-frequency x-intercept where the imaginary impedance equals zero.

Scattering measurements were performed with a multiangle X-ray scattering system (MAXS) equipped with a Nonius FR 591 rotating-anode Cu X-ray generator operated at 40 kV and 85 mA. The beam was focused with Confocal Max-Flux optics in an integral vacuum system. Scattering data were collected over a 1 h interval using a Bruker Hi-Star multiwire detector with a sample-to-detector distance of 11, 54, and 150 cm. 2-D data reduction and analysis were performed using Datasqueeze software.

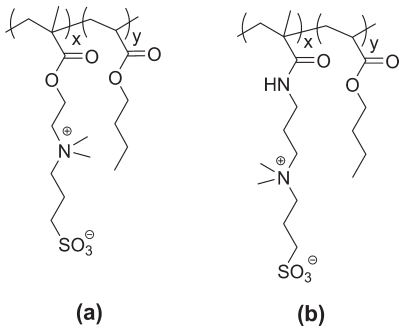

Figure 1. Structure of zwitterionic copolymers: (a) PnBA-*co*-PSBMA and (b) PnBA-*co*-PSBMAm.

Table 1. Relative Molecular Weights of Zwitterionomers

copolymer	M_n (g/mol)	M_w (g/mol)	M_w/M_n
$PnBA_{94}$-*co*-$PSBMA_6$	165 000	460 000	2.78
$PnBA_{91}$-*co*-$PSBMA_9$	141 000	324 000	2.31
$PnBA_{91}$-*co*-$PSBMA_9$	105 000	265 000	2.51
$PnBA_{94}$-*co*-$PSBMAm_6$	214 000	519 000	2.42
$PnBA_{90}$-*co*-$PSBMAm_{10}$	134 000	344 000	2.65
$PnBA_{90}$-*co*-$PSBMAm_{10}$	141 000	295 000	2.11
$PnBA_{87}$-*co*-$PSBMAm_{13}$	94 100	259 000	2.75

Results and Discussion

Synthesis and Characterization of Zwitterionomers. Zwitterionic copolymers containing 6 and 9 mol % of SBMA or 6, 10, and 13 mol % of SBMAm (Figure 1) were synthesized using free radical copolymerization in DMSO to afford high molecular weight zwitterionomers. ^{1}H NMR spectroscopy confirmed the copolymer composition matched the feed within 1 mol % for all compositions. Copolymer molecular weights were determined using SEC in DMF with 0.01 M LiBr, and values relative to polystyrene standards are reported in Table 1. Dynamic light scattering was performed prior to SEC to indentify the optimal solvent composition and ensure minimal aggregation in DMF with LiBr. The purified polymers were soluble in chloroform and membranes were solution cast from chloroform into Teflon molds to form ductile, free-standing membranes. Copolymer membranes were dried thoroughly under vacuum at 80 °C to remove residual chloroform and absorbed water and then stored in a desiccator prior to swelling or analysis.

Previous DMA studies showed that PnBA-*co*-PSBMA and PnBA-*co*-PSBMAm zwitterionomer membranes exhibited two-phase morphologies indicative of ionic aggregation.[12,26,28] In our current study, X-ray scattering results

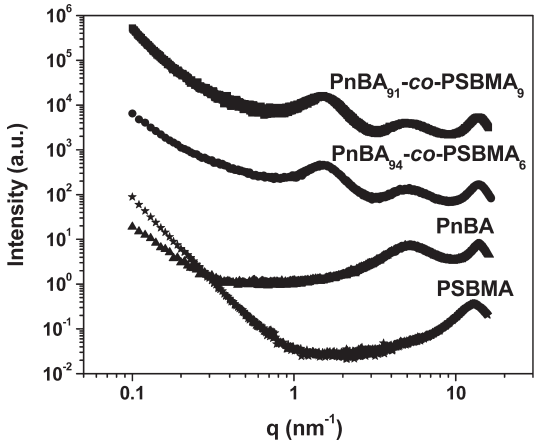

Figure 2. X-ray scattering intensity vs scattering vector (q) for PnBA-*co*-PSBMA (9 and 6 mol %), PnBA, and PSBMA.

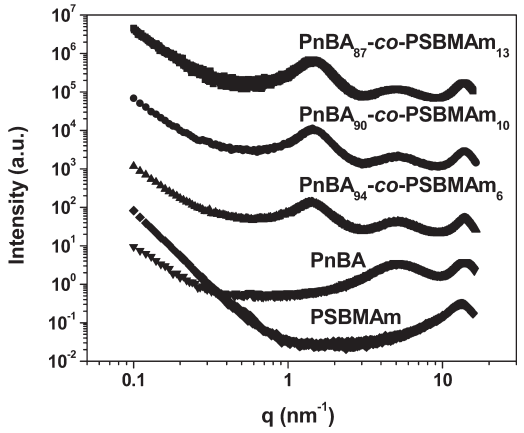

Figure 3. X-ray scattering intensity vs scattering vector (q) for PnBA-*co*-PSBMAm (13, 10, and 6 mol %), PnBA, and PSBMAm.

revealed the bulk morphology of zwitterionic membranes, and all samples exhibited isotropic rings in the 2D scattering patterns. Figure 2 shows the multiangle X-ray scattering profiles for a series of PnBA-*co*-PSBMA copolymers and corresponding homopolymers as a log−log plot of scattering intensity versus the scattering vector q. Three primary scattering peaks were observed for the zwitterionic copolymers. A peak at ~14 nm^{-1} was observed for the zwitterionomers as well as both homopolymers. This peak is characteristic of amorphous polymers and is attributed to local ordering of pendant chains.[29] A peak at ~5 nm^{-1} was observed in both PnBA and the zwitterionomers, and this peak was attributed to local ordering of chain segments or the distance between polymer main chains, in accordance with assignments made earlier by Miller and Boyer for amorphous poly(*n*-alkyl methacrylates) and poly(*n*-alkyl acrylates).[29]

The broad peak at ~1.5 nm^{-1} was observed only in the zwitterionic copolymers and may be classified as an ionomer peak, which confirmed the presence of a second ionic phase that was observed in DMA.[12,26] The ionomer peak is typically broad in random ionomers due to a range of spacings between ionic domains. This scattering peak at low q corresponded to a Bragg spacing (d) of ~4 nm and exhibited a slight dependence on ion content as the peak maximum shifted slightly to higher q with increasing SBMA content. This spacing was consistent with other zwitterionic copolymers[8,11] as well as random ionomers[13,30−32] reported in the literature. Similar results were also obtained for the PnBA-*co*-PSBMAm copolymers as shown in Figure 3. Ionomer peak positions as a function of zwitterionomer content and the corresponding d spacings are summarized in Table 2.

Table 2. Summary of Scattering Peaks and *d*-Spacings for Zwitterionomers, PnBA, and Zwitterionic Homopolymers

polymer composition	peak position (nm^{-1})			d spacing, ionomer peak (nm)
$PnBA_{91}$-*co*-$PSBMA_9$	1.52	4.92	13.7	4.13
$PnBA_{94}$-*co*-$PSBMA_6$	1.45	4.92	13.7	4.33
$PnBA_{87}$-*co*-$PSBMAm_{13}$	1.54	4.97	13.7	4.08
$PnBA_{90}$-*co*-$PSBMAm_{10}$	1.46	4.97	13.7	4.30
$PnBA_{94}$-*co*-$PSBMAm_6$	1.39	4.97	13.7	4.52
PnBA		5.2	13.7	
PSBMA			12.8	
PSBMAm			13.2	

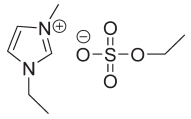

Figure 4. Chemical structure of 1-ethyl-3-methylimidazolium ethylsulfate (EMIm ES).

Swelling of Zwitterionomers with Ionic Liquid. While the affinities of polybetaines for water and inorganic salts are well documented, their interactions with ILs have received little attention.[33] The IL chosen for this study was 1-ethyl-3-methylimidazolium ethylsulfate (EMIm ES), as shown in Figure 4. EMIm ES is an inexpensive and commercially available water-miscible IL with a melting point of −65 °C and bulk conductivity (σ) of 3.82 mS cm^{-1} at 298 K. The low melting point and good conductivity at 298 K made EMIm ES a good candidate for initial studies in the room temperature application of IL-swollen zwitterionic membranes for electrical devices.

Copolymer membranes were placed in scintillation vials of EMIm ES and stored in a desiccator at constant RH for the duration of the swelling study. The original dry mass was recorded, and the uptake of IL was measured as a function of weight gain over a period of several months. Initial studies of membrane swelling in EMIm ES were performed on all SBMA and SBMAm copolymers that contained 6−13 mol % zwitterion. These preliminary data showed a significant effect of zwitterion loading on the amount of IL uptake. Very low swelling levels were observed for copolymers with 6 mol % zwitterion, and the IL uptake was difficult to accurately measure using gravimetric techniques. Copolymers with 9 or 10 mol % zwitterion content showed moderate swelling, while the 13 mol % SBMAm copolymer exhibited the largest swelling capacity. These results showed that the IL had a large affinity for the polar zwitterionic phase, leading to higher swelling levels at increasing zwitterion concentrations. The inability to swell the membranes with a significant amount of ionic liquid at zwitterion contents of only 6 mol % suggested the absence of a percolated ionic phase throughout the membranes, which limited the transport of ionic liquid.

This preliminary study also highlighted the influence of sample dimensions, sample history, and swelling conditions on the reproducibility of swelling measurements. When swelling was conducted in closed containers on the benchtop without control of temperature or humidity, much larger increases in weight were observed reaching > 100%, suggesting a synergistic effect of water with IL in the swelling process. Also, drastic differences in the kinetics of swelling were observed among membranes of various sizes and thicknesses. Therefore, constant conditions for film formation,

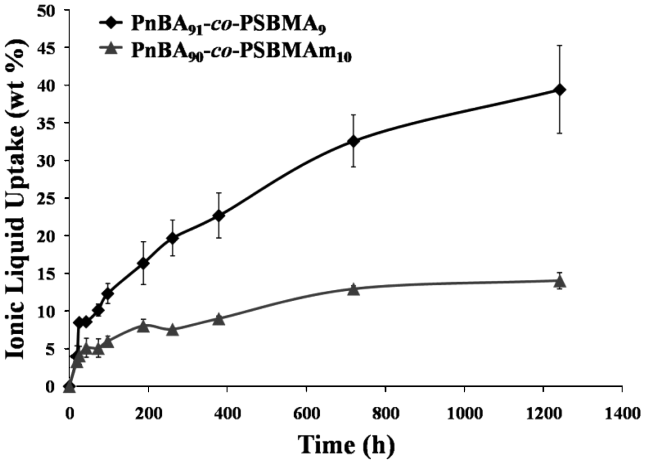

Figure 5. Swelling behavior of $PnBA_{91}$-*co*-$PSBMA_9$ and $PnBA_{90}$-*co*-$PSBMAm_{10}$ in EMIm ES as a function of time.

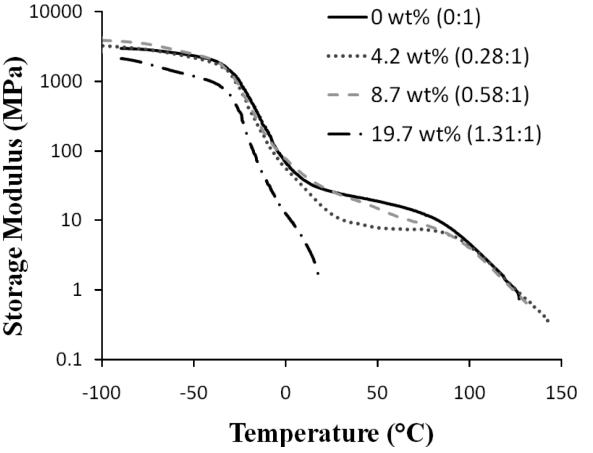

Figure 6. DMA storage modulus as a function of temperature for $PnBA_{91}$-*co*-$PSBMA_9$ (M_w 265 000 g/mol) at various levels of swelling in EMIm ES: 0 wt % (0:1 mol EMIm ES:mol SB), 4.2 wt % (0.28:1), 8.7 wt % (0.58:1), and 19.7 wt % (1.31:1).

annealing, and swelling were adopted to minimize variations in swelling times.

For the purpose of this study, we chose to focus on $PnBA_{91}$-*co*-$PSBMA_9$ and $PnBA_{90}$-*co*-$PSBMAm_{10}$ in more depth in order to maintain a good comparison between these two zwitterionomer classes. Swelling results for the zwitterionomers containing ~10 mol % betaine functionality were plotted as percent weight gain versus time, as shown in Figure 5. It is readily apparent that despite similar zwitterion loadings, molecular weights, and solid-state properties, these membranes exhibited significantly different swelling behaviors. The maximum uptake observed for $PnBA_{91}$-*co*-$PSBMA_9$ within the period of this study was 40 wt %, while $PnBA_{90}$-*co*-$PSBMAm_{10}$ plateaued at 14 wt %. Small differences in film thickness (0.23 and 0.28 mm) were not sufficient to explain this drastic difference in behavior. We propose that the presence of synergistic hydrogen bonding in the amide-linked zwitterionomer provided additional ionic aggregate stability, causing a decrease in the overall IL uptake within the polar ionic phase. Further studies to confirm this hypothesis are needed. This controlled swelling data were used to determine the swelling time for copolymer membranes to reach various swelling levels; comprehensive characterization of the influence of IL uptake on membrane mechanical properties, morphology, and conductivity was performed.

Mechanical Properties of Ionic Liquid Swollen Membranes. The thermal and mechanical properties of both neat and swollen zwitterionic membranes were characterized using DMA. Gauthier and co-workers reported DMA behavior of PnBA-*co*-PSBMA of varying compositions.[28] At low zwitterionic contents, two thermal transitions were observed in DMA as well as the presence of a rubbery plateau due to physical ionic cross-linking within the ionic domains. Similar behavior was observed for $PnBA_{91}$-*co*-$PSBMA_9$ (M_w 265 000) in the absence of IL as shown in Figure 6 (0 wt %). The first transition corresponded to the T_g of the ion-poor matrix phase of the copolymer, i.e., PnBA. The second transition, which occurs between 80 and 90 °C at the end of the rubbery plateau, may be attributed to the T_g of the ion-rich phase.

Upon swelling with EMIm ES, the matrix phase T_g decreased within experimental error from −26 °C without IL present to −28 °C at 19.7 wt % swelling. However, the rubbery plateau region and the ion-rich phase T_g revealed substantial differences with increasing IL content. At low swelling levels below 10 wt % IL (0, 4.2, and 8.7 wt % IL in Figure 6), corresponding to less than 0.65 mol EMIm ES per mol SB, mechanical properties remained virtually unchanged within the experimental error. The only differences observed at these lower IL contents occurred in the rubbery plateau region, where a decrease in rubbery modulus did not follow a systematic trend with increasing IL content. Additional dynamic mechanical analyses at swelling levels below 10 wt % are required to understand the rubbery plateau behavior.

In stark contrast to the behavior at low swelling levels, a rubbery plateau was not observed and flow occurred below 25 °C for zwitterionic copolymer membranes at the highest IL swelling level studied of 19.7 wt % IL (1.31 mol IL:mol SBMA). The insignificant change in T_g of the PnBA phase at increasing levels of IL uptake indicated that the water-miscible IL did not significantly influence the hydrophobic PnBA matrix. The disappearance of the rubbery plateau at higher swelling levels indicated that the ion-rich domains were preferentially swollen with IL. Galin and co-workers[25] studied the plasticization of zwitterionic copolymers consisting of a PnBA matrix with plasticizers of drastically different polarities. Dibutyl phthalate (DBP), which has a high affinity for PnBA, was incorporated homogeneously into both phases of the copolymer. However, incorporation of ethylammonium nitrate (EAN) or water, which have high affinities for the dipolar zwitterions, resulted in the plasticization of only the ion-rich phase.[25] For IL swelling, EMIm ES was expected to have a high affinity for the ionic domains, and only the matrix T_g as determined using DMA was observed at 19.7 wt % EMIm ES. This drastic decrease in the T_g of the zwitterionic phase is also in agreement with the observed plasticization behavior of ionomers.[34,35] Polar plasticizers are known to selectively incorporate into the ionic phase (multiplets), which reduces the electrostatic interaction between ion pairs and increases the mobility of the polymer chains attached to the ionomer multiplets.[35]

Similar mechanical properties for swelling levels up to ~10 wt % were also observed for $PnBA_{90}$-*co*-$PSBMAm_{10}$ (M_w 295 000). Storage modulus as a function of temperature is plotted in Figure 7 for $PnBA_{90}$-*co*-$PSBMAm_{10}$ at swelling levels of 0, 5.4, and 10.1 wt % EMIm ES. The observed similarity of mechanical properties at low swelling levels in both copolymer membranes suggested the presence of a critical IL uptake level, and significant changes in polymer morphology and mechanical performance were expected

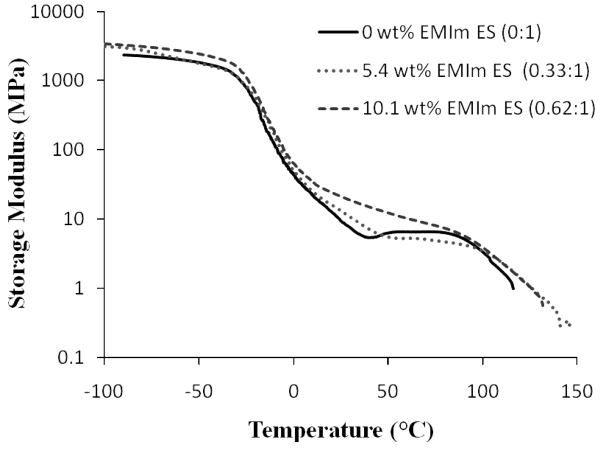

Figure 7. Storage modulus vs temperature profiles for $PnBA_{90}$-*co*-$PSBMAm_{10}$ (M_w 295 000 g/mol) at various swelling levels.

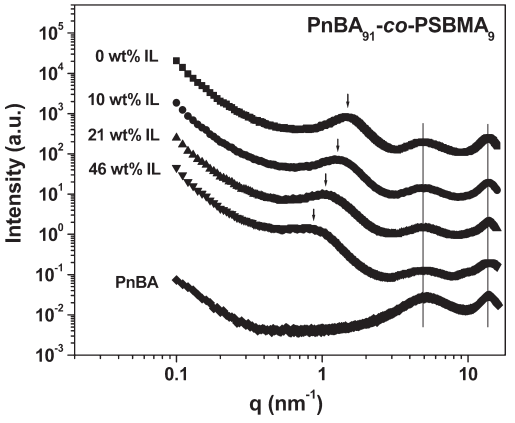

Figure 8. X-ray scattering intensity vs scattering vector (q) for $PnBA_{91}$-*co*-$PSBMA_9$ at increasing levels of IL content showing the shift in the ionomer peak; PnBA is also plotted for comparison of the high q region.

above this critical level. This critical uptake level was estimated between 10.1 and 19.7 wt % (0.62−1.31 mol IL:SB), and the drastic change in behavior at 19.7 wt % may indicate the exact transition occurred at a composition closer to 10.1 wt %. This assumption is further correlated with ionic conductivity data presented later. Galin et al.[25] suggested the presence of a transition or plateau region between 0.7 and 1.5 mol EAN/mol SB in the plasticization of PnBA-*co*-PSBMAm copolymers, which was tentatively related to observed behavior in the plasticization of ionomers with polar diluents. A large shift in Bragg spacing to lower q in the SAXS profile was attributed to a rearrangement of the ionic domains, presumably involving the coalescence of ionic regions into fewer, larger aggregates.[13,25] We studied the relevance of this morphological change to zwitterionic membranes with IL using X-ray scattering analysis as a function of IL content.

Morphological Changes in the Presence of Ionic Liquid. Swelling of the membrane zwitterionic domains was expected to cause changes in the zwitterionomer morphology, especially in the ionomer peak of the SAXS profile. X-ray scattering profiles, plotted as intensity vs scattering vector q on a log−log plot, at various IL swelling levels of $PnBA_{91}$-*co*-$PSBMA_9$ are shown in Figure 8. The scattering profile in the absence of IL is identical to Figure 2. The ionomer peak systematically shifted to lower q as the ionic liquid content increased, i.e., 1.49 nm^{-1} at 0 wt % to 0.87 nm^{-1} at 46 wt % EMIm ES. This highest swelling level corresponded to

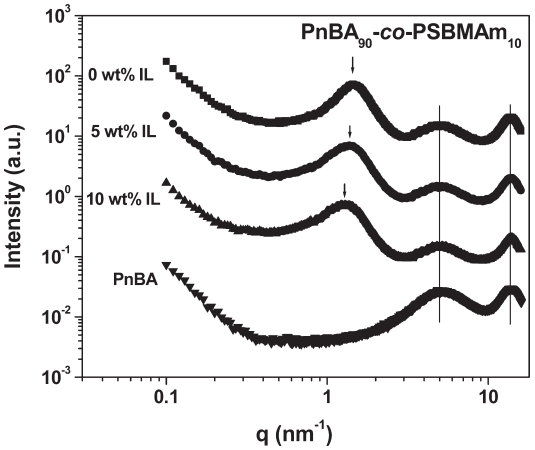

Figure 9. X-ray scattering intensity vs scattering vector (q) for $PnBA_{90}$-*co*-$PSBMAm_{10}$ at three swelling levels of IL showing a shift in the ionomer peak; PnBA is also plotted for comparison of the high q region.

3.13 mol EMIm ES per mol of SB functionality. The other two peaks in the SAXS profiles at 4.9 and 13.7 nm^{-1} remained unchanged with increasing IL content. The shift of the ionomer peak and the lack of change in the peak representing the ordering of the polymer matrix (∼4.9 and 13.7 nm^{-1}) confirmed our hypothesis that the water-miscible EMIm ES swelled the zwitterionic domains preferentially without affecting the matrix phase and supported the dynamic mechanical behavior. Furthermore, a similar shift of the ionomer peak with increasing IL content was observed for $PnBA_{90}$-*co*-$PSBMAm_{10}$, as shown in Figure 9 for swelling levels of 0, 5, and 10 wt % EMIm ES. The scattering peak locations, corresponding Bragg spacings of the ionomer peaks, and the ionic liquid contents are summarized in Table 3.

Gierke et al. first proposed a cluster-network model for Nafion ionomers, and then Eisenberg[13] and others modified this general model to account for various other experimental observations for ionomers. In general, these models feature a spherical ionic cluster phase within a continuous matrix phase.[36] On the basis of this model, the angular position of the ionomer peak in the SAXS profile represents the average spacing between centers of ionic clusters. Swelling studies of ionomers with polar diluents have supported this proposed morphology. Gierke et al. observed an increase in the average intercluster spacings with increasing water content in Nafion.[36] Leo and co-workers[20,37] also observed similar increases upon swelling Nafion with two different ionic liquids. The increase in spacing was larger for swelling with the water-miscible IL 1-ethyl-3-methylimidazoliumtrifluoromethanesulfonate (EMI-Tf) than for the hydrophobic IL 1-ethyl-3-methylimidazolium bis(trifluoromethanesulfonyl)-imide (EMI-Im). Similarly, a sizable increase in the spacing was observed for swelling of zwitterionomers with EMIm ES in the present work. This increase in intercluster spacing likely corresponded to an increase in cluster size through plasticization with IL. An increase in d spacing was generally observed for many ionomers in the literature, and the multiplet-cluster morphology is well-documented. Unfortunately, modeling of the SAXS data for spherical ionic domains using the Kinning−Thomas model[38] was not in agreement with our hypothesized swelling behavior, as explained earlier. Future microscopy imaging of the ionic domains is needed to further understand the structure of the ionic domains and changes in domain size with increasing IL content.

Table 3. Summary of Scattering Peaks and *d*-Spacings for Zwitterionomers Swollen in IL

copolymer	IL content (wt %)	IL content (mol IL:mol SB)	peak position (nm^{-1})			*d* spacing (nm)
$PnBA_{91}$-*co*-$PSBMA_9$	0	0:1	1.49	4.91	13.7	4.22
	10	0.64:1	1.28	4.91	13.7	4.91
	15	1.0:1	1.07	ND	ND	5.87
	21	1.40:1	1.06	4.91	13.7	5.93
	46	3.13:1	0.87	4.91	13.7	7.22
$PnBA_{90}$-*co*-$PSBMAm_{10}$	0	0:1	1.43	5.04	13.7	4.39
	5	0.31:1	1.38	5.04	13.7	4.55
	10	0.62:1	1.28	5.04	13.7	4.91
PnBA	0	0		5.18	13.7	

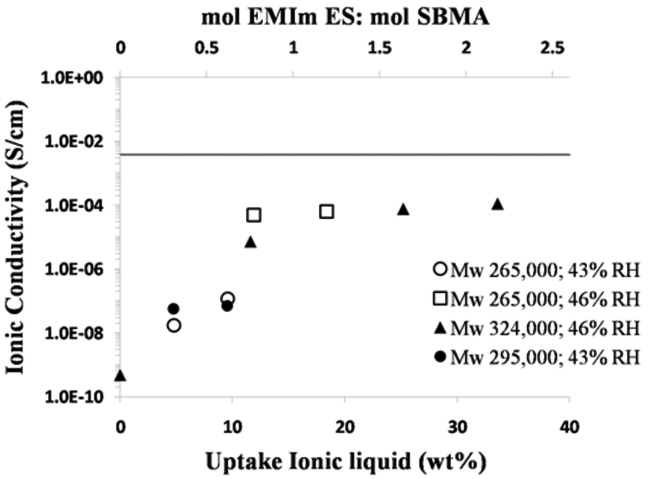

Figure 10. Semilog plot of ionic conductivity vs IL uptake for $PnBA_{91}$-*co*-$PSBMA_9$ (○, ▲, □) and $PnBA_{90}$-*co*-$PSBMAm_{10}$ (●) membranes in EMIm ES.

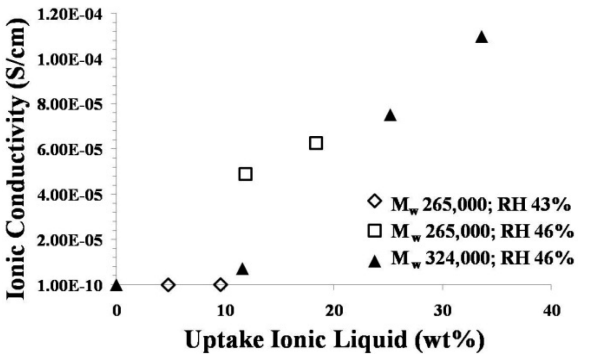

Figure 11. Ionic conductivity of $PnBA_{91}$-*co*-$PSBMA_9$ membranes in EMIm ES, plotted as a function of IL uptake, revealing a critical uptake transition.

Effect of IL Swelling on Membrane Conductivity. Electrical properties of the neat and IL-swollen zwitterionic copolymer membranes were analyzed using electrical impedance spectroscopy. Ionic conductivity was calculated from the resistance, as revealed from the *x*-intercept of a semicircle fit on a Nyquist plot. Figure 10 shows the ionic conductivity as a function of both wt % IL uptake and molar ratio of IL to SBMA for $PnBA_{91}$-*co*-$PSBMA_9$. Conductivity values of the neat membranes were expected to be very low due to the absence of mobile counterions; ionic conductivities on the order of 10^{-9} S cm^{-1} are typical for synthetic polymers without diluent. Ionic conductivity increased with the addition of EMIm ES, reaching values on the order of 10^{-4} S cm^{-1} at 10−20 wt % or 0.7−1.2 mol IL:SBMA and approaching the conductivity of pure EMIm ES, 3.82 mS cm^{-1}.

The same conductivity results were also plotted on a linear scale to reveal the presence of a critical uptake point, above which a sizable change in conductivity was observed (Figure 11). IL uptake between 0 and ∼10 wt % resulted in very small differences in ionic conductivity, while a drastic increase occurred above 11.6 wt % IL. A critical uptake value between 10 and 12 wt % was inferred from impedance analysis, in good agreement with the small influence of IL below 10 wt % on mechanical properties in DMA. More data points are necessary to further pinpoint the exact critical uptake, but there is reasonable evidence from both impedance spectroscopy and DMA that this change in behavior occurred just above 10 wt %.

Ionic conductivities of $PnBA_{90}$-*co*-$PSBMAm_{10}$ membranes containing 5 and 10 wt %, 0.31 and 0.62 mol IL:SB, respectively, were also measured under the same conditions as $PnBA_{91}$-*co*-$PSBMA_9$ (265 000 g/mol), as shown in Figure 10. Ionic conductivities for both zwitterionomer families were comparable, measured within 1 order of magnitude at equivalent swelling levels. These results correlated well to DMA results, where similar mechanical properties were also observed at equivalent swelling levels for both zwitterionomer families.

Impedance spectroscopy and subsequent resistance values are highly dependent on the environmental conditions during sample testing. Small differences in relative humidity of the testing chamber led to noticeable changes in ionic conductivity, as seen for the membrane of M_w 265 000 g/mol for two testing periods with differences of 3% RH. Testing with 3% higher RH led to conductivities about a half of an order of magnitude larger than expected based on the increasing trend. This trend is consistent with a higher water content for the membranes with larger conductivities. Ionic conductivity is also highly dependent upon sample preparation, water content, sample history, and membrane−electrode contact. Relatively good agreement between membranes of different molecular weights and testing conditions was encouraging and indicated reproducibility of results.

Conclusions

Copolymers containing sulfobetaine-type zwitterions in a poly(*n*-butyl acrylate) matrix were synthesized using conventional free radical copolymerization in DMSO. X-ray scattering revealed a two-phase morphology of the neat membranes, with a characteristic ionomer peak at ∼1.5 nm^{-1}. Zwitterionic membranes containing 9 or 10 mol % sulfobetaine were solution cast from chloroform and swollen in the water-miscible IL, EMIm ES. Zwitterion structure influenced the swelling behavior of the membranes, where IL uptake in ester-linked zwitterionic films was more than double the uptake for amide-linked zwitterionic films over equivalent swelling times. DMA revealed the disappearance of the rubbery plateau as the ion-rich phase was plasticized with increasing amounts of IL above 10 wt % IL. SAXS analysis showed a systematic shift to lower *q* with increasing IL uptake, without corresponding changes in scattering

profiles at $q \sim 4.9$ nm^{-1}, corresponding to the local ordering of the polymer matrix chains. These results confirmed that the IL was preferentially swollen into the ionic domains without affecting the morphology of the nonpolar matrix. Ionic conductivity also increased with IL uptake, approaching the conductivity of pure IL. DMA and conductivity results for $PnBA_{91}$-*co*-$PSBMA_9$ indicated a critical uptake of IL near 11 wt %, above which significant changes in mechanical properties and increases in conductivity occurred. Ester- and amide-linked zwitterionomers at equivalent IL swelling levels exhibited very similar mechanical and electrical properties below 10 wt % IL. The observed critical IL content of ~11 wt %, or ~0.7 mol of EMIm ES per mol of zwitterion functionality, is in agreement with Galin's hypothesis that a morphological change occurred at higher swelling levels.[25] Microscopy imaging is needed to fully understand the structure and changes in domain size and shape with increasing IL content.

Acknowledgment. This material is based upon work supported by the U.S. Army Research Laboratory and the U.S. Army Research Office under Grant W911NF-07-1-0339.

References and Notes

(1) Galin, M.; Chapoton, A.; Galin, J. C. *J. Chem. Soc., Perkin Trans.* **1993**, *2*, 545–553.
(2) Koberle, P.; Laschewsky, A. *Macromolecules* **1994**, *27*, 2165–2173.
(3) Galin, M.; Marchal, E.; Mathis, A.; Meurer, B.; Soto, Y. M. M.; Galin, J. C. *Polymer* **1987**, *28*, 1937–1944.
(4) Galin, M.; Marchal, E.; Mathis, A.; Galin, J. C. *Polym. Adv. Technol.* **1997**, *8*, 75–86.
(5) Kudaibergenov, S.; Jaeger, W.; Laschewsky, A. *Adv. Polym. Sci.* **2006**, *201*, 157–224.
(6) Lowe, A. B.; McCormick, C. L. *Chem. Rev.* **2002**, *102*, 4177–4189.
(7) Mathis, A.; Zheng, Y. L.; Galin, J. C. *Makromol. Chem., Rapid Commun.* **1986**, *7*, 333–337.
(8) Mathis, A.; Zheng, Y. L.; Galin, J. C. *Polymer* **1991**, *32*, 3080–3085.
(9) Ehrmann, M.; Galin, J. C. *Polymer* **1992**, *33*, 859–865.
(10) Ehrmann, M.; Galin, J. C.; Meurer, B. *Macromolecules* **1993**, *26*, 988–993.
(11) Ehrmann, M.; Mathis, A.; Meurer, B.; Scheer, M.; Galin, J. C. *Macromolecules* **1992**, *25*, 2253–2261.
(12) Ehrmann, M.; Muller, R.; Galin, J. C.; Bazuin, C. G. *Macromolecules* **1993**, *26*, 4910–4918.
(13) Eisenberg, A.; Hird, B.; Moore, R. B. *Macromolecules* **1990**, *23*, 4098–4107.
(14) Lu, J. M.; Yan, F.; Texter, J. *Prog. Polym. Sci.* **2009**, *34*, 431–448.
(15) Luo, S. C.; Zhang, Z. X.; Yang, L. *Chin. Sci. Bull.* **2008**, *53*, 1337–1342.
(16) Galinski, M.; Lewandowski, A.; Stepniak, I. *Electrochim. Acta* **2006**, *51*, 5567–5580.
(17) Yang, S. C.; Yoon, H. G.; Lee, S. S.; Lee, H. *Mater. Lett.* **2009**, *63*, 1465–1467.
(18) Mishra, A.; Fischer, M. K. R.; Bauerle, P. *Angew. Chem., Int. Ed.* **2009**, *48*, 2474–2499.
(19) Duncan, A. J.; Leo, D. J.; Long, T. E. *Macromolecules* **2008**, *41*, 7765–7775.
(20) Bennett, M. D.; Leo, D. J.; Wilkes, G. L.; Beyer, F. L.; Pechar, T. W. *Polymer* **2006**, *47*, 6782–6796.
(21) Ding, J.; Zhou, D.; Spinks, G.; Wallace, G.; Forsyth, S.; Forsyth, M.; MacFarlane, D. *Chem. Mater.* **2003**, *15*, 2392–2398.
(22) Lu, W.; Fadeev, A. G.; Qi, B.; Smela, E.; Mattes, B. R.; Ding, J.; Spinks, G. M.; Mazurkiewicz, J.; Zhou, D.; Wallace, G. G.; MacFarlane, D. R.; Forsyth, S. A.; Forsyth, M. *Science* **2002**, *297*, 983–987.
(23) Vidal, F.; Plesse, C.; Teyssie, D.; Chevrot, C. *Synth. Met.* **2004**, *142*, 287–291.
(24) Bennett, M. D.; Leo, D. J. *Sens. Actuators, A* **2004**, *115*, 79–90.
(25) Galin, M.; Mathis, A.; Galin, J. C. *Macromolecules* **1993**, *26*, 4919–4927.
(26) Brown, R. H.; Hunley, M. T.; Allen, M. H.; Long, T. E. *Polymer* **2009**, *50*, 4781−4787.
(27) Gauthier, M.; Carrozzella, T.; Penlidis, A. *J. Polym. Sci., Part A: Polym. Chem.* **2002**, *40*, 511–523.
(28) Gauthier, M.; Carrozzella, T.; Snell, G. *J. Polym. Sci., Part B: Polym. Phys.* **2002**, *40*, 2303–2312.
(29) Miller, R. L.; Boyer, R. F. *J. Polym. Sci., Polym. Phys.* **1984**, *22*, 2021–2041.
(30) Moore, R. B.; Gauthier, M.; Williams, C. E.; Eisenberg, A. *Macromolecules* **1992**, *25*, 5769–5773.
(31) Benetatos, N. M.; Winey, K. I. *Macromolecules* **2007**, *40*, 3223–3228.
(32) van der Mee, M. A. J.; l'Abee, R. M. A.; Portale, G.; Goossens, J. G. P.; van Duin, M. *Macromolecules* **2008**, *41*, 5493–5501.
(33) Strehmel, V.; Wetzel, H.; Laschewsky, A.; Moldenhauer, E.; Klein, T. *Polym. Adv. Technol.* **2008**, *19*, 1383–1390.
(34) Bazuin, C. G.; Eisenberg, A. *J. Polym. Sci., Part B: Polym. Phys. Ed.* **1986**, *24*, 1137–1153.
(35) Kim, J.-S.; Roberts, S. B.; Eisenberg, A.; Moore, R. B. *Macromolecules* **1993**, *26*, 5256–5258.
(36) Gierke, T. D.; Munn, G. E.; Wilson, F. C. *ACS Symp. Ser.* **1982**, *180*, 195–216.
(37) Bennett, M.; Leo, D. *Proc. SPIE-Int. Soc. Opt. Eng.* **2005**, *5759*, 506–517.
(38) Kinning, D. J.; Thomas, E. L. *Macromolecules* **1984**, *17*, 1712–1718.